RSC Advances

ROYAL SOCIETY OF CHEMISTRY

www.rsc.org/advances

Structure-Property Studies of P-Triarylamine-Substituted Dithieno[3,2-*b*:2',3'-*d*]phospholes

Hannes Puntscher[a,b,†], Paul Kautny[a,†], Berthold Stöger[c], Antoine Tissot[d], Christian Hametner[a], Hans R. Hagemann[d], Johannes Fröhlich[a], Thomas Baumgartner[b,*], and Daniel Lumpi[a,*]

[a] Institute of Applied Synthetic Chemistry, Vienna University of Technology, Getreidemarkt 9/163, A-1060 Vienna, Austria

[b] Department of Chemistry & Centre for Advanced Solar Materials, University of Calgary, 2500 University Dr. NW, Calgary AB, T2N 1N4, Canada

[c] Institute of Chemical Technologies and Analytics, Vienna University of Technology, Getreidemarkt 9/164, A-1060 Vienna, Austria

[d] Département de Chimie Physique, Université de Genève, 30, quai E. Ansermet, 1211 Geneva 4, Switzerland

* ttbaumga@ucalgary.ca, daniel.lumpi@tuwien.ac.at

† *contributed equally to this work*

Table of contents entry

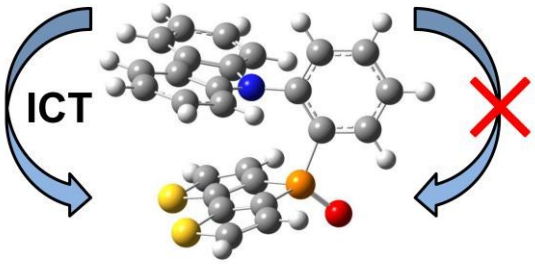

The photo-physical and theoretical investigation of 10 novel donor-acceptor materials sheds new light on charge transfer in dithienophosphole oxide derivatives.

Abstract

The synthesis of 10 novel P-substituted dithienophosphole oxide compounds applying phenylcarbazole and indolocarbazole donors is presented. Based on photo-physical and theoretical investigations, the study reveals that the pyramidal geometry of the phosphorus allows for the synthesis of charge transfer materials by introducing strong exocyclic donor groups but suppresses intramolecular charge transfer below a certain donor strength threshold, which is an appealing structural feature for the design of donor-acceptor materials. The triplet energies of the phenylcarbazole based compounds are in the range of 2.49 eV – 2.65 eV, sufficiently high for potential applications as host materials in PhOLEDs. By contrast, the introduction of indolocarbazole, the weakest employed donor, yields materials exhibiting a significantly higher triplet energy of up to 2.87 eV and a remarkably low singlet-triplet splitting (0.18 eV). In addition an interesting example of an intramolecular electronic through-space interaction has been observed for the *ortho*-linked phenylcarbazole derivative.

1) Introduction

The development of functional π-conjugated organic materials for applications in organic electronics such as organic light emitting diodes (OLEDs),[1-3] organic field effect transistors (OFETs),[4-6] organic photovoltaics (OPVs)[7, 8] or sensors[5, 6] is a steadily evolving field of research due to the appealing possibility of tailoring the organic materials' intrinsic electronic properties by subtle modifications of their molecular framework.[9] The incorporation of main group elements such as B,[10-12] Si,[13-15] Se,[16] Te[17] or P[18-22] has proven to be a particularly valuable tool for designing materials featuring, e.g., highly interesting optical properties, inaccessible through purely hydrocarbon-based compounds.

In this context, the dithieno[3,2-*b*:2',3'-*d*]phosphole scaffold (Figure 1) has been thoroughly investigated as novel platform for functional materials in the last decade.[23] The electron lone pair of the phosphorus atom within the phosphole structure has high s-character that hinders efficient interaction with the π-system.[23] Therefore, the aromaticity of phospholes is diminished compared to other five-membered heterocycles, such as pyrrole, thiophene or furan. Nevertheless, interactions between the σ*-orbital of the exocyclic bond and the π*-system of the ring lead to a certain degree of aromaticity and a high polarizability of the phosphole system.[23, 24] The resulting high tunability of the photo-physical and electro-chemical properties by chemical modification[22, 23, 25] suggested the utility of this versatile building block for the fields of luminescent materials,[26-31] polymers,[32-34] coordination chemistry[26, 35] and self-organizing materials.[36, 37] In particular, oxidation of the phosphorus center is an appealing strategy to significantly enhance the electron-accepting properties of the dithieno[3,2-*b*:2',3'-*d*]phosphole moiety,[21, 24] which enables the application of this scaffold in donor-acceptor type materials.

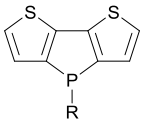

Figure 1. Molecular scaffold of dithieno[3,2-*b*:2',3'-*d*]phosphole

Donor-acceptor materials are of specific interest for applications due to the possibility to selectively influence photo-physical and electro-chemical characteristics by intramolecular charge transfer (ICT)[2, 3, 38-40] as well as bipolar charge transport properties in electronic devices.[39, 41] Thus, the interaction of the molecular donor and acceptor subunits is of crucial importance. Phosphine oxide derivatives have been widely applied as functional materials in OLEDs.[21] Particularly bipolar host materials for phosphorescent OLEDs (PhOLEDs) comprising phosphine oxide and carbazole[42-44] or triphenylamine[45, 46] moieties were exhaustively investigated due to limited conjugation *via* the phosphine oxide as result of its tetrahedral geometry.[21] Moreover, the coordination geometry of the phosphorus atom in the five-membered phosphole ring offers new opportunities to control electronic and photo-physical characteristics.[22-24] Whereas direct substitution of the thiophene moieties allows for full conjugation with the main scaffold, the pyramidal structure of the PC_3 fragment prevents π-conjugation of the exocyclic substituent with the dithieno[3,2-*b*:2',3'-*d*]phosphole core.

Recently, the influence of exocyclic donor groups on the properties of dithieno[3,2-*b*:2',3'-*d*]phosphole based donor-acceptor materials has been investigated[29-31] revealing efficient charge transfer from the donor to the dithieno[3,2-*b*:2',3'-*d*]phosphole oxide core.[29] Herein we report on the synthesis and characterization of a new series of dithieno[3,2-*b*:2',3'-*d*]phosphole oxides with phenylcarbazole or indolo[3,2,1-*jk*]carbazole substituents as exocyclic donor moieties; the experimental results have been correlated with DFT calculations. In order to further elucidate the

influence of the donor-acceptor interaction on the photo-physical properties of the whole system, the influence of various substitution patterns, as well as planarization of the donor was investigated.

2) Results and Discussion

2.1) Synthesis and Characterization

Intrigued by the initial studies on systems with an exocyclic triphenyl amine substituent,[29] this work focuses on less electron-donating aryl amines such as phenylcarbazole (PCz; with *ortho*-, *meta*- and *para*-substitution pattern) and indolo[3,2,1-*jk*]carbazole (ICz). Due to the increasing contribution of the nitrogen lone pair to the π-system of the pyrrole-like rings in the planarized triarylamine (TAA) subunits, the donor strength is reduced in the order triphenylamine > phenylcarbazole > indolocarbazole.[47] To circumvent possible insolubility issues as a result of the incorporation of increasingly planarized structural motives, the *n*-butyl substituted species **3ai**-**ei** were synthesized in addition to target molecules **3a**-**e** without alkyl substituents (Scheme 1). Furthermore, in the case of the *meta*-linked phenylcarbazole, *t*-butyl substituents were introduced at the 3- and 6-position of the carbazole unit in order to investigate the influence of these substituents on molecular properties, but to also enhance the electro-chemical stability of the latter.[48] Following established procedures, the synthesis of the dithienophospholes was accomplished by lithiation of the corresponding dibromobithiophenes **2** or **2i**, followed by conversion of the lithiated species with $TAAPCl_2$ **1a**-**e** at low temperature (Scheme 1). The $TAAPCl_2$ starting materials were prepared from the corresponding bromides (TAABr) via suitably adapted literature procedures[29] and were applied without further purification. For a streamlined synthetic process, the resulting trivalent phosphorus compounds were not isolated but directly oxidized by addition of excess H_2O_2 yielding target compounds **3a**-**3ei** in moderate to low yields after column chromatography.

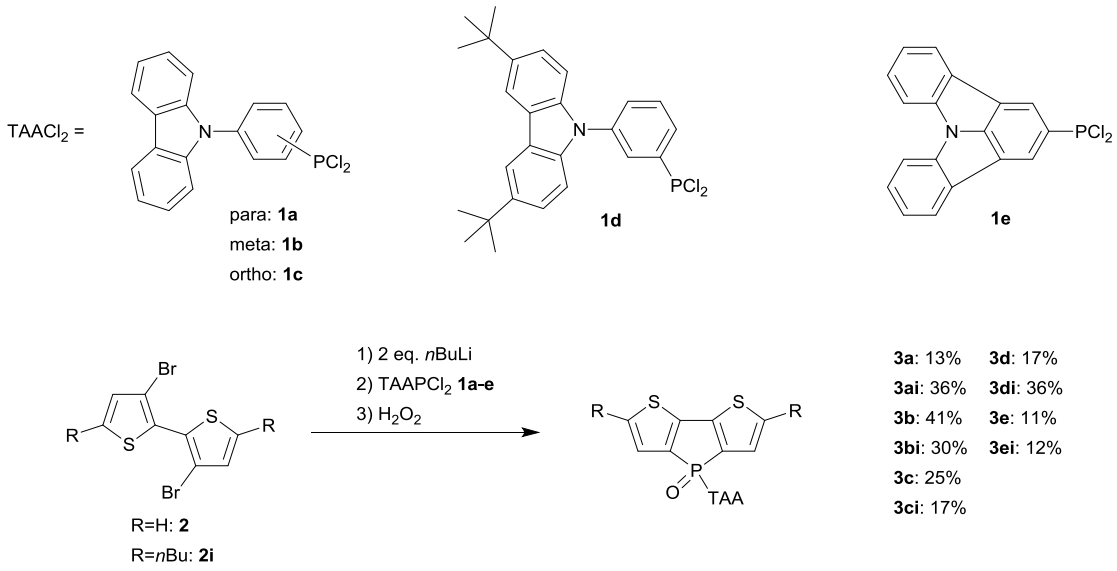

Scheme 1. Synthetic pathways towards carbazole and indolo[3,2,1-*jk*]carbazole functionalized dithienophosphole oxides **3a**-**3ei**.

The carbazole-based compounds **3a**, **3b** and **3d** exhibited ^{31}P NMR chemical shifts at δ = 16.2, 17.8 and 18.0 ppm, respectively, that are shifted somewhat upfield compared to the corresponding triphenyl amine-substituted dithienophosphole oxide (cf.: 19.1 ppm).[29] In contrast, indolocarbazole-substituted **3e** showed a slightly downfield-shifted ^{31}P NMR resonance at δ = 22.2 ppm that is, however, in line with related systems exhibiting exocyclic polyaromatic hydrocarbon (PAH) substituents.[30] By contrast, *ortho*-derivative **3c** featured a significantly upfield-shifted ^{31}P NMR chemical shift at δ = 12.9 ppm compared to its congeners **3a** and **3b**, indicating a distinctively different chemical environment of the phosphorus atom for this particular configuration. In all cases, the *n*-butyl substituents at the dithienophosphole core led to slightly (1-3 ppm) downfield-shifted resonances, which is in accordance with previous findings.[29] In addition, the successful formation of target compounds **3a**-**3ei** was also confirmed by ^{1}H and ^{13}C NMR spectroscopy, as well as high-resolution mass spectroscopy (HRMS).

Moreover, single crystals of **3c**[49] suitable for X-ray crystallography were obtained from a CD_2Cl_2 solution upon slow evaporation of the solvent at room temperature

(Figure 2). Bond lengths and angles within the dithienophosphole oxide scaffold are in good accordance with previously reported P-phenyl substituted derivatives.[29, 30] Elongated double bonds and shortened single bonds indicate a high degree of conjugation of the planar scaffold (largest distance of 0.0457(10) Å from the least squares (L.S.) plane observed for the C6 atom). Notably, the carbazole unit deviates distinctly from planarity (distance of the C17 atom from the L.S. plane of 0.1211(10) Å). The most striking feature is the alignment of the dithienophosphole and the carbazole units (Figure 2 (left)). Due to the *ortho*-linkage on the phenylene linker, the carbazole is forced in close vicinity to the dithienophosphole unit resulting in a parallel orientation (angle of L.S. planes of 8.26(2)°) of the two subunits. The shortest interatomic contact between both units is only 3.2424(12) Å (C4—C26) hinting toward strong intramolecular π-π interactions. In contrast, no such intermolecular interactions are observed with neighboring molecules (Figure 2 (right)).

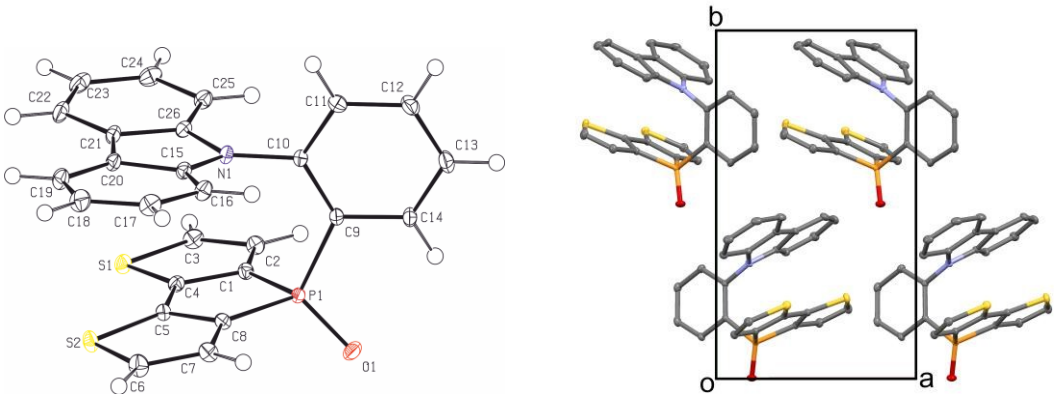

Figure 2. Molecular structure of **3c** (left) in the solid state (50% probability level, H atoms are represented by white spheres of arbitrary radius); Selected bond lengths [Å] and angles [□]: P1-C2: 1.8062(9); P1-C6: 1.7979(9); P1-C9: 1.8167(8); C1-C2: 1.4220(14); C1-C4: 1.3824(12); C2-C3: 1.3680(13); C4-C5: 1.4526(14); C5-C8: 1.3825(12); C6-C7: 1.3689(13); C7-C8: 1.4216(14); C2-P1-C6: 92.32(4); C2-P1-C9: 110.51(4); C6-P1-C9: 109.14(4); C2-P1-O1: 166.99(4); C6-P1-O1: 116.38(4); C9-P1-O1: 110.25(4); Packing of **3c** (right) in the single crystal viewed along the c-axis (H atoms were omitted for clarity).

The particular spatial arrangement of the *ortho*-linked derivatives **3c** and **3ci** was verified in solution *via* NMR spectroscopy. Following a complete signal assignment

(ESI) using standard 2D methods, 1D and 2D NOESY spectra were recorded (ESI). Significant NOE enhancement of the carbazole *ortho*-proton upon irradiation of both of the thiophene signals (and *vice versa*) clearly indicates close vicinity of the respective moieties in compound **3c**. A similar result was obtained for the same carbazole-H and the remaining thiophene proton for **3ci**. Thus, parallel alignment of carbazole and dithienophosphole ring systems in the *ortho*-bridged molecules **3c** and **3ci** can be assumed in solution as well.

2.2) Photo-physical Investigations

In order to investigate the photo-physical properties of the newly developed materials, UV/VIS absorption and photo-luminescence spectra were recorded in dilute CH_2Cl_2 solutions; results are summarized in Table 1. The absorption spectra (Figure 3 (top), ESI) exhibit specific features of both chromophores – the dithienophosphole and carbazole moieties. Whereas the low wavelength region is dominated by well-resolved transitions at approximately 292, 326 and 338 nm, typical for phenylcarbazoles,[50] broad absorption bands, which can be attributed to the dithienophosphole unit,[27, 35, 51] are observed at higher wavelengths (350-400 nm). Notably, peaks arising from the carbazole donors are insensitive to the presence/absence of the *n*-butyl groups at the dithienophosphole. In contrast, installation of the *t*-butyl groups at the 3- and 6-position leads to red-shifted carbazole absorption peaks for **3d** and **3di**. Related transitions are observed for the indolocarbazole-based materials **3e** and **3ei**. The absorption bands arising from the indolocarbazole unit are slightly blue-shifted compared to those of carbazole, which is in accordance with previously reported results.[52] Similarly, the absorption of the dithienophosphole moieties are not influenced by the triarylamines, with exception of **3c** and **3ci**, but the *n*-butyl substituents lead to a red-shift of the broad

dithienophosphole peak. The optical bandgaps determined from the absorption onset of **3a**/**b**/**d**/**e** are located in a narrow range between 3.04 – 3.06 eV. The absorption onsets of *n*-butyl-substituted **3ai**/**3bi**/**3di**/**3ei** are shifted to energies between 2.85 - 2.87 eV likely due to the "+I" effect of the donating butyl substituent (*vide infra*). However, most striking is the observation that absorption onsets of *ortho*-derivatives **3c** and **3ci** are red-shifted by nearly 0.1 eV compared to their respective congeners. The same tendencies are found in emission spectra (Figure 3 (bottom), ESI). Whereas **3a**/**b**/**d**/**e** exhibit featureless emission maxima around 454 nm, the emission of the *n*-butyl substituted materials **3ai**/**bi**/**di**/**ei** is red-shifted by approximately 30 nm, due to the donor-effect if the alkyl groups (*vide infra*), while the emission maxima of **3c** and **3ci** are located at 471.5 and 495.5 nm, respectively. Remarkably, the emission of **3a**/**b**/**d**/**e** is identical to the purely phenyl-substituted dithienophosphole oxide (453 nm).[32] Therefore, the addition of electron-rich aryl amines does not seem to influence the emission properties of the materials. This is also supported by the DFT calculations that identify the dithienophosphole $\pi*$-system as the LUMO for all species with largely comparable HOMO-LUMO energy gaps (*vide infra*). From these findings – as well as the fact that absorption and emission properties are independent of the kind of the adjacent subunit and linkage mode (with the exception of *ortho*-linkage) – we conclude that the electronic coupling of both chromophores is basically suppressed by linkage *via* the phosphorus atom. This finding is in disagreement with previous findings concerning triphenyl amine substituted dithienophosphole oxides that exhibit pronounced ICT,[29] but can be attributed to the fact that the donor-strength of the aryl amines applied in this study is significantly decreased compared to triphenyl amine.[52] Therefore, the pyramidal nature of the phosphorus allows for the synthesis of charge transfer materials based on strong exocyclic donor groups but suppresses ICT below a certain donor strength threshold.

This appealing structural feature for the design of donor-acceptor materials has also been confirmed *via* the DFT calculations (*vide infra*).

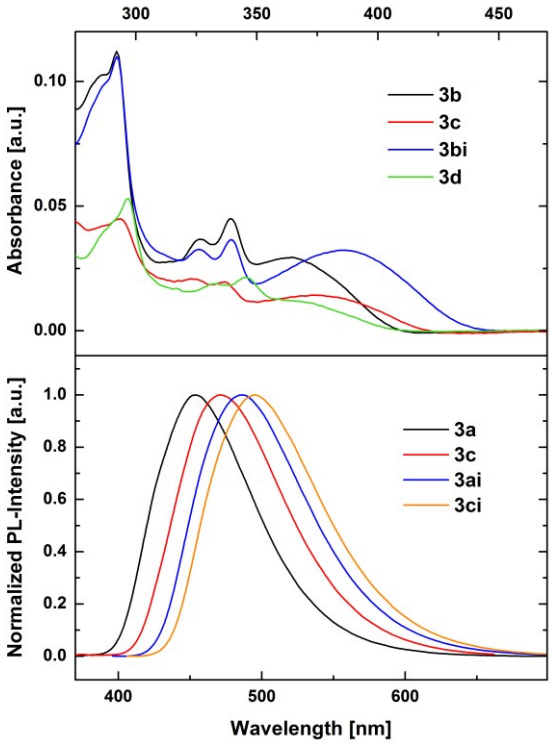

Figure 3. Absorption spectra of **3b**, **3c**, **3d** and **3bi** (top) and normalized PL spectra of **3a**, **3c**, **3ai** and **3ci** (bottom). All spectra were recorded from 5 μM solution in DCM at r.t.

In contrast to the photo-physical properties of all other investigated materials in this study, those of the *ortho*-derivatives **3c** and **3ci** are distinctly different, indicating the presence of electronic interactions between the carbazole and dithienophosphole moieties. Due to the fact that these interactions are absent in *para*-linked **3a** and **3ai,** which exhibit the highest degree of conjugation between the two molecular subunits, electronic exchange *via* the phenylene linker can be ruled out. However, the close vicinity of the planar carbazole and dithienophosphole, which has been confirmed by NOE measurements, suggests through-space interaction of the aromatic groups that are also revealed by the theoretical calculations (*vide infra*).

Bipolar organic materials exhibiting limited ICT have received great attention in recent years due to potential applications as host materials for transition metal complexes in PhOLEDs.[39, 53] The incorporation of phosphorescent triplet emitters in electro-optical devices overcomes the limitation of purely fluorescent emitter and theoretically allows for 100% internal quantum efficiency.[54] These phosphorescent emitters have to be dispersed in an organic matrix for efficiency reasons. One major requirement of such host materials are high triplet energy (E_T) values in order to confine the excited states on the emitter. However, the combination of donor and acceptor subunits within one molecule lowers the E_T *via* ICT.[39, 53] Therefore, research focuses on the design and synthesis of donor-acceptor materials with decreased interaction between the molecular subunits. In this regard we investigated the E_Ts of the developed materials. The E_Ts were determined in frozen (solid) toluene solutions at 77 K from the highest vibronic transition of the delayed emission, and decrease in the order of *para* (**3a** = 2.65 eV / **3ai** = 2.60 eV) > *meta* (**3b** = 2.56 eV / **3bi** = 2.51 eV) > *ortho* (**3c** = 2.53 eV / **3ci** = 2.49 eV), respectively. These values are sufficiently high for applications as host materials in green and red PhOLEDs.[39] While the additional *t*-butyl substituents at the carbazoles in **3d** and **3di** do not influence the energy levels, all of the *n*-butyl-substituted compounds feature slightly decreased E_Ts compared to the unsubstituted dithienophospholes. However, the influence of the *n*-butyl substituents on the E_Ts is lower compared to the corresponding optical bandgap E_S (Figure 4). Notably, the ICz-substituted compound **3e** features a significantly higher E_T of 2.87 eV (Figure 5), rendering the application in blue PhOLEDs possible. In contrast to all other materials **3e** exhibits vibronically well resolved phosphorescence (Figure 5, ESI), indicating a localized T_1 (^{3}LE) state.[55] The transition from a charge transfer T_1 (^{3}CT) state to a ^{3}LE in case of **3e** can be explained by the weaker donor strength of the ICz moiety destabilizing the ^{3}CT and

thus might be the explanation for the significantly increased E_T of **3e**. In addition, the low singlet-triplet splitting of 0.18 eV makes this material particularly interesting. Recently, Adachi and coworkers introduced bipolar compounds with low singlet-triplet splitting as highly efficient electro-optical materials by means of thermally activated delayed fluorescence (TADF) due to thermal up-conversion of excited triplet states to singlet states.[56] Thus, the investigated approach of attaching exocyclic donors to dithienophosphole oxides *via* the pyramidal coordinated phosphorus may provide a new design concept for efficient TADF materials.

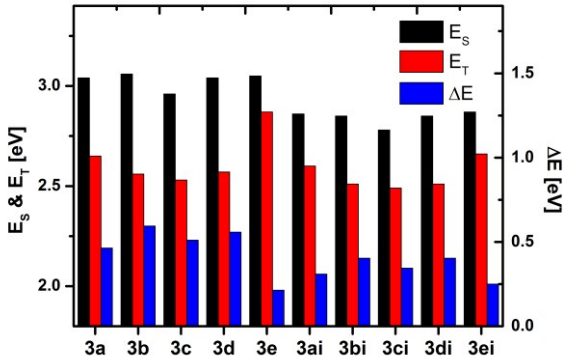

Figure 4. Singlet energies (E_S), triplet energies (E_T) and singlet-triplet splitting of all synthesized materials.

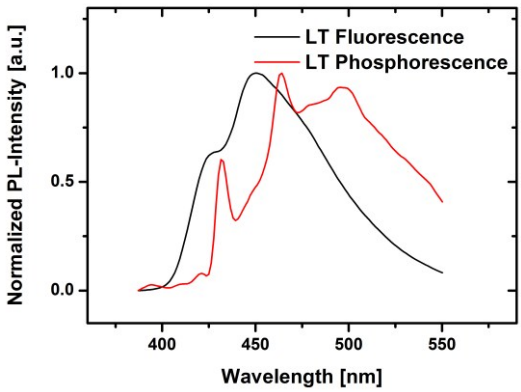

Figure 5. Low temperature fluorescence and phosphorescence spectra of **3e** recorded at 77 K.

Table 1. Photo-physical properties of the synthesized materials.

Compound	λ_{abs} [nm]	λ_{em} [nm]	E_S [eV][a]	E_T [eV][b]
3a	392/326/338/366(sh[c])	454	3.04	2.65
3b	292/327/339/364	454.5	3.06	2.56
3c	293/323/337/374	471.5	2.96	2.53
3d	297/333/337/368(sh[c])	456	3.04	2.57
3e	288/310/323/360	451.5	3.05	2.87
3ai	292/326/338/386	486.5	2.86	2.60
3bi	292/326/339/386	486.5	2.85	2.51
3ci	293/324/337/397	495.5	2.78	2.49
3di	297/333/346/386	487.5	2.85	2.51
3ei	286/308/323/367/389(sh[c])	482	2.87	2.66

[a]Estimated from the absorption onset. [b] Estimated from the highest energy vibronic transition in toluene at 77 K. [c]Shoulder.

2.3) Theoretical Calculations

In order to provide some deeper understanding of the experimentally determined photo-physics of the materials in this study, we have performed Density-Functional Theory (DFT) calculations at the B3LYP/6-31+G(d) level of theory using the Gaussian 09 suite of programs.[57] In order to save computing time, the butyl groups in the 'i' series of compounds were replaced with methyl substituents and the corresponding species are denominated as **3(a-e)i'**. The DFT data generally support the experimentally determined features, with most compounds showing similar photo-physics, and the *ortho*-carbazole substituted species being distinct from their congeners. As a common denominator, the LUMO orbitals of all investigated species comprise the $\pi*$-system of the dithienophosphole scaffold, with the presence of the *n*-butyl groups being reflected in commonly increased energy levels by approximately 0.15 eV compared to their H-substituted relatives (Table 2). Another common denominator is the fact that the HOMO, HOMO-1 and HOMO-2 levels of all compounds are fairly close in energy for each compound (ΔE ~ 0.4 eV) and consequently relevant for the observed experimental photo-physics. These orbitals respectively represent - to varying extents - the π-systems of the dithienophosphole and the triaryl amine scaffolds, as well as the π-bridge between the units in **3a,b,d,e** and **3(a,b,d,e)i'** (ESI). It should also be mentioned in this context that the HOMO for **3a,b,d** and **3(a,b,d)i'** represents the π-system of the carbazole substituents with largely comparable energy levels (E_{HOMO} ~ -5.7 eV), a feature that has been confirmed by cyclic voltammetric (CV) measurements (Table 2).

Notably, the presence of the butyl substituents in the 2- and 6-positions of the dithienophospholes raises the energy of this unit's π-system, which leads to a switch in the orbital order with the π-system of the corresponding carbazole unit. The

calculations suggest that the raised level of the dithienophosphole π-system in the *para*- and *meta*-carbazole species (HOMO-1, instead of HOMO-2 in **3a,b,d**), in combination with the lowered LUMO levels is responsible for the red-shifted photo-physics of the 'i'-series of compounds. This also indicates a reduced electronic communication between the two sub-chromophores. The effect of the *t*-butyl substituents in **3d** and **3di'** is reflected in the increased energies of the respective HOMO levels at E_{HOMO} ~ -5.5 eV (CV: **3d**: -5.54 eV; **3di**: -5.53 eV).

Table 2. Orbital energies and character of the frontier orbitals.

Compd.	E_{HOMO-2} [eV] (character)	E_{HOMO-1} [eV] (character)	E_{HOMO} [eV] (character)	E_{LUMO} [eV] (character)	E^{ox} [V] CV	E_{HOMO} [eV] CV
3a	-6.14 (π-S_2P)	-6.13 (π-cbz)	-5.76 (π-cbz-ph)	-2.24 (π*-S_2P)	0.91	-5.71
3b	-6.13 (π-S_2P)	-6.12 (π-cbz)	-5.75 (π-cbz-ph)	-2.24 (π*-S_2P)	0.90	-5.70
3c (syn)	-6.10 (π-S_2P-cbz)	-5.93 (π-S_2P-cbz)	-5.78 (π-S_2P-cbz)	-2.08 (π*-S_2P)	0.86	-5.66
3d	-6.10 (π-S_2P)	-5.96 (π-cbz)	-5.55 (π-cbz-ph)	-2.21 (π*-S_2P)	0.74	-5.54
3e	-6.47 (π-icz)	-6.11 (π-S_2P-icz)	-5.92 (π-S_2P-icz)	-2.09 (π*-S_2P)	0.96	-5.76
3ai	-6.10 (π-cbz)	-5.82 (π-S_2P-cbz)	-5.69 (π-S_2P-cbz)	-2.09 (π*-S_2P)	0.94	-5.74
3bi	-6.09 (π-cbz)	-5.78 (π-S_2P)	-5.72 (π-cbz-ph)	-2.09 (π*-S_2P)	0.88	-5.68
3ci'-syn	-6.05 (π-cbz)	-5.80 (π-S_2P-cbz)	-5.55 (π-S_2P-cbz)	-1.93 (π*-S_2P)	0.85	-5.65
3ci'-anti	-5.93 (π-cbz)	-5.72 (π-S_2P-cbz)	-5.67 (π-S_2P-cbz)	-2.08 (π*-S_2P)	---	---
3di	-5.93 (π-cbz)	-5.75 (π-S_2P)	-5.51 (π-cbz-ph)	-2.06 (π*-S_2P)	0.73	-5.53
3ei	-6.41 (π-icz)	-6.02 (π-icz)	-5.61 (π-S_2P)	-1.95 (π*-S_2P)	0.78	-5.58

S_2P: dithienophosphole; cbz: carbazole; ph: phenylene; icz: indolocarbazole; E^{ox}: oxidation potential relative to Fc/Fc^+

In the case of **3e** and **3ei'**, the observed slight blue shift is the result of increased LUMO levels, compared to those of **3a,b,d(i')**. However, the donor-effect of the methyl substituent is evident in the respective HOMO levels (-5.92 eV for **3e** vs. -5.61 eV for **3ei'**). This particular electrochemical behavior has been confirmed by CV measurements. In contrast to all other pairs of molecules the aliphatic substituent at

the dithienophosphole leads to an increase of the HOMO energy in case of **3ei** (-5.58 eV) compared to **3e** (-5.76 eV). Remarkably, the orbital sequence and electronic contributions to the frontier orbitals of the indolocarbazole-substituted species (particularly for **3ei**), approach those of the PAH-substituted species,[30] clearly reflecting the effect of the diminishing donor-strength of the exocyclic substituent. The DFT data for the latter suggest only limited ICT present in this system, which is in fact absent in the PAH-relatives.

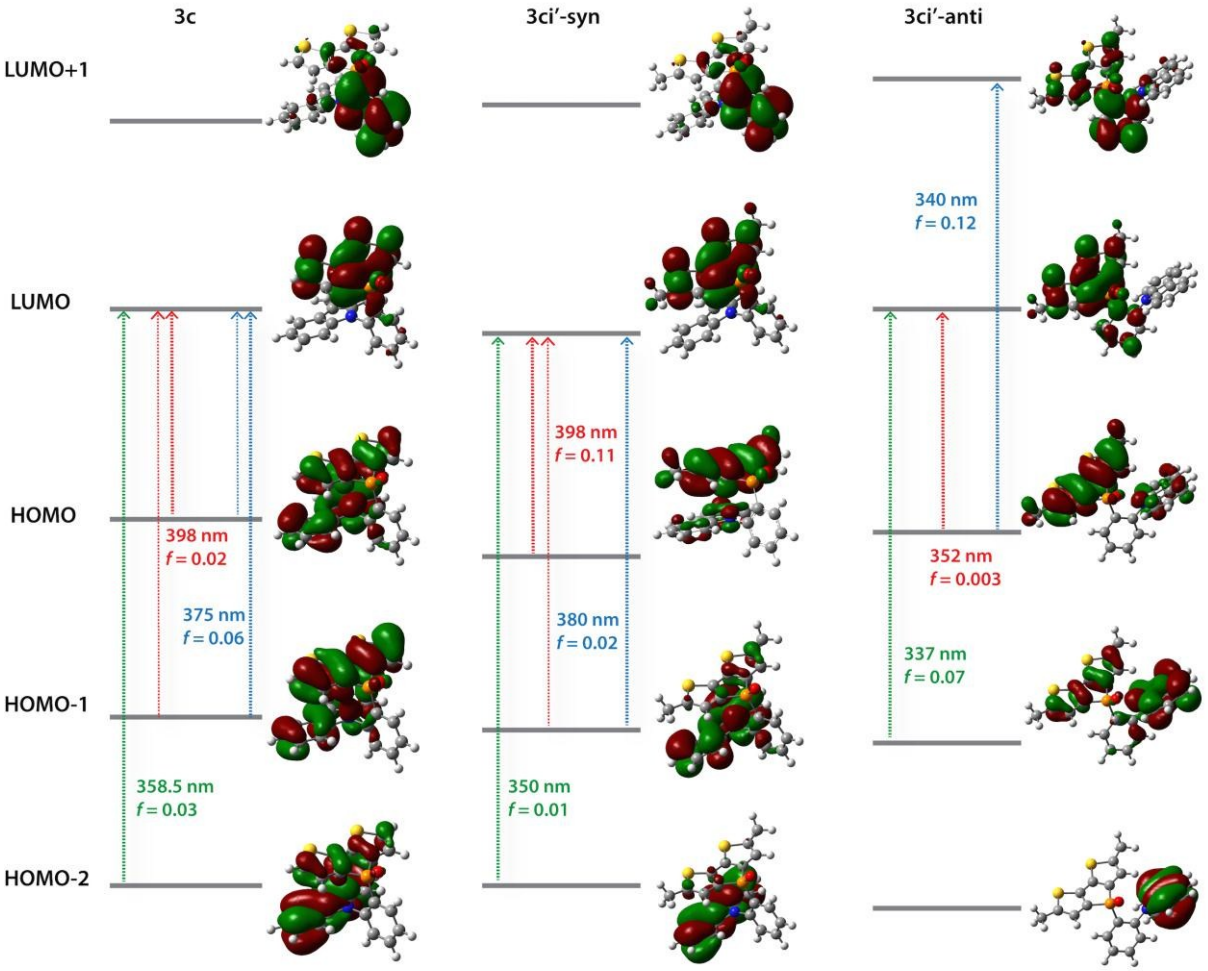

Figure 6. TD-DFT calculation data for **3c, 3ci'-syn** and **3ci'-anti** showing notable transitions as well as their intensity (*f* = oscillator strength). Thickness of arrow indicates weight to transition.

As mentioned above, the photo-physics of the *ortho*-substituted congeners were found to be distinct from those of the rest of the series. For this reason we have

performed some more detailed studies on these species, including time-dependent (TD) DFT calculations at the B3LYP/6-31+G(d) level of theory. To establish the presence of electronic through-space interactions, we have included a conformer of **3ci'**, in which the two sub-chromophores exhibit an *anti*-configuration, without the possibility of through-space interactions. In fact, the DFT calculations for **3ci'-anti** provide orbital energies, that are not much different from those of the *para*- and *meta*-linked relatives, albeit with the HOMO largely comprising the dithienophosphole π-system (with the addition of the phenylene bridge), and the HOMO-1 and HOMO-2 showing increasing contribution for the carbazole π-system with diminishing contribution from the dithienophosphole scaffold (Figure 6).

However, while there is certainly also a resemblance between the shape/contributions of these orbitals in **3ci'-anti** with those of the two *syn*-configured conformers **3c** and **3ci'-syn**, the close proximity of the dithienophosphole and carbazole π-systems opens up through-space interactions in the latter. This is already reflected in orbital shapes and energies that deviate by about 0.1-0.2 eV from those of the other relatives (ESI, Table S2). However, a much clearer picture is provided by the relevant transitions obtained from the TD-DFT calculations that show distinct differences between the *syn*- and *anti*-conformers (Figure 6). For **3ci'-anti** the lowest energy absorption, corresponding to an excitation HOMO→LUMO occurs at 352 nm, however with very low oscillator strength (*f* = 0.0029). Other transitions of note include HOMO→LUMO+1 (340 nm; *f* = 0.1201), HOMO-1→LUMO (337 nm; *f* = 0.0722), with the most intense transition at 295 nm (*f* = 0.1744) corresponding to HOMO-1→LUMO+1 (the π*-system of the phenylene bridge). In the case of the *syn*-conformers **3c** and **3ci'-syn**, the lowest energy transitions appear around 400 nm, in line with the experimental data, representing a mix of HOMO→LUMO (95%) and

HOMO-1→LUMO (5%) (*f* = 0.0154) for **3c** and HOMO→LUMO (2%) and HOMO-1→LUMO (96%) (*f* = 0.1133) for **3ci'-syn**. Both species show two further transitions of note, respectively, that appear at 375 nm for **3c** (HOMO-1→LUMO (92%), HOMO→LUMO (4%); *f* = 0.0608), 380 nm for **3ci'-syn** (HOMO-1→LUMO; *f* = 0.0208), as well as 358.5 nm for **3c** (HOMO-2→LUMO; *f* = 0.0313) and 350 nm for **3ci'-syn** (HOMO-2→LUMO; *f* = 0.0121). These calculations are in line with the experimental data and rule out the *anti*-conformation to be relevant for the observed photo-physics and support the presence of through-space interactions resulting from *syn*-configuration.

3) Experimental Section

3.1) General Information

All reactions were carried out under nitrogen atmosphere, employing standard Schlenk techniques. Reagents and solvents were purchased from commercial suppliers and used without further purification unless noted otherwise. Anhydrous solvents were absolutized by an MBraun solvent purification system prior to use. NMR spectra were recorded on Bruker Avance-II/-III 400 MHz Spectrometers; for compounds **3c** and **3ci** 2D NMR spectra for complete signal assignment (COSY, HSQC, HMBC) as well as 1D and 2D NOESY spectra were obtained on a Bruker Avance IIIHD 600 MHz spectrometer equipped with a Prodigy BBO cryo probe. A Thermo Scientific LTQ Orbitrap XL hybrid FTMS (Fourier Transform Mass Spectrometer) equipped with a Thermo Fischer Exactive Plus Orbitrap (LC-ESI+) and a Shimadzu IT-TOF Mass Spectrometer were used for high resolution mass spectrometry. UV/VIS absorption and fluorescence emission spectra were recorded in DCM solutions (5 μM) with a Perkin Elmer Lambda *750* spectrometer and an Edinburgh FLS920, respectively. Time resolved experiments were obtained using a Quantel Brilliant tripled Nd-YAG laser (355 nm, 20 Hz repetition rate, pulse width ~5 ns). Spectra were measured using a SPEX 270 monochromator equipped with both photomultiplier and CCD. This set-up is controlled using a home-built Labview-based program which allows using different instruments such as photon counting, oscilloscope, and additional mechanical shutters. For the measurement of the triplet emission, a mechanical shutter was triggered by the pulsed laser. A pretrigger period of 0.5 ms was followed by a 1 ms aperture and a rest time of 300 – 500 ms allowed obtaining the measurements shown in the ESI. The slit of the monochromator was also opened further (up to 0.5 mm) to measure the triplet emission. Cyclic voltammetry was performed using a three electrode configuration consisting of a Pt

working electrode, a Pt counter electrode and an Ag/AgCl reference electrode and a PGSTAT128N, ADC164, DAC164, External, DI048 potentiostat provided by Metrohm Autolab B.V with ferrocenium-ferrocene (Fc/Fc^{+}) as standard. Measurements were carried out in a 0.5 mM solution in anhydrous DCM with Bu_4NBF_4 (0.1 M) as supporting electrolyte. The solutions were purged with nitrogen for 15 minutes prior to measurement. HOMO energy levels were calculated from the onset of the oxidation peaks. The onset potential was determined by the intersection of two tangents drawn at the background and the rising of the oxidation peaks. HOMO levels were calculated according to the equation $HOMO = -(4.8+E^{ox})$, where E^{ox} is the oxidation potential relative to Fc/Fc^{+}.

3.2) Synthetic Details

Dibrominated bithiophenes **2**[58] and **2i**[31] were synthesized as described in literature. Dichlorophosphanes **1a**-**e** were prepared in analogy to a previously published procedure from the corresponding brominated precursors and were used crude without any further purification.[29]

General procedure for the synthesis of TAA-substituted dithieno[3,2-*b*:2´,3´-*d*]phospholes. The synthesis of TAA-substituted dithieno[3,2-*b*:2´,3´-*d*]phospholes was accomplished according to established procedures.[26, 27, 29, 32, 33, 59] To a solution of **2**/**2i** (1 eq.) and TMEDA (2 eq.) in dry diethylether or THF (~0.25 M) under nitrogen atmosphere was added *n*-BuLi (2.5 M in hexane, 2 eq.) dropwise at -78 °C. The reaction mixture was stirred at -78 °C before a solution of dichlorophosphane **1a**/**b**/**c**/**d**/**e** (1 eq.) in dry THF (0.05-0.1 M) was slowly added. Subsequently the resulting mixture was allowed to warm to room temperature quickly, stirred for one hour and the solvent was removed under vacuum. The residue was dissolved in chloroform and excess of water and H_2O_2 (30%, 0.5-1 mL/mmol) was added. After stirring for 1.5 hours the organic phase was dried over $MgSO_4$ before the solvent was removed and the crude product was purified by column chromatography.

4-(4-(9*H*-Carbazol-9-yl)phenyl)-4*H*-phospholo[3,2-*b*:4,5-*b*']dithiophene 4-oxide (3a). Starting from **2** (1.00 g, 3.1 mmol) and TMEDA (0.94 mL) in diethylether, *n*-BuLi (2.47 mL, 2.5 M), **1a** (0.75 g, 2.2 mmol, 0.71 eq.) and H_2O_2 (30%, 2 mL) product **3a** (130 mg, 0.29 mmol, 13%) was obtained as light yellowish solid after column chromatography (silica, ethyl acetate); undefined impurities (approx.. 5-10%) were not separable from **3a** by repeated column chromatography. $^{31}P\{^1H\}$ NMR (162 MHz, CD_2Cl_2): δ = 16.2 (s) ppm. ^1H NMR (400 MHz, CD_2Cl_2): δ = 8.14 (d, J=7.6 Hz, 2H), 7.95 (dd, J=12.7, 8.3 Hz, 2H), 7.68 (dd, J=8.3, 2.4 Hz, 2H), 7.47-7.39 (m, 6H), 7.32-7.25 (m, 4H) ppm. $^{13}C\{^1H\}$ NMR (100 MHz, CD_2Cl_2): δ = 146.5 (d, J_{CP}=24.3 Hz),

142.1 (d, J_{CP}=3.5 Hz), 140.8 (s), 139.4 (d, J_{CP}=112.3 Hz), 133.2 (d, J_{CP}=12.1 Hz), 129.4(4) (d, J_{CP}=108.1 Hz), 129.4(1) (d, J_{CP}=14.9 Hz), 127.5 (d, J_{CP}=13.0 Hz), 126.7 (s), 126.4 (d, J_{CP}=14.5 Hz), 124.2 (s), 121.0 (s), 120.9 (s), 110.3 (s) ppm. Calculated: m/z 453.04054 $[M]^+$, 454.04837 $[M+H]^+$, 476.03031 $[M+Na]^+$. Found: MS (ESI): m/z 453.03978 $[M]^+$, 454.04737 $[M+H]^+$, 476.02944 $[M+Na]^+$.

4-(4-(9*H*-Carbazol-9-yl)phenyl)-2,6-dibutyl-4*H*-phospholo[3,2-*b*:4,5-*b*']dithiophene 4-oxide (3ai). Starting from **2i** (0.80 g, 1.8 mmol) and TMEDA (0.58 mL) in diethylether, *n*-BuLi (1.46 mL, 2.5 M), **1a** (0.63 g, 1.8 mmol) and H_2O_2 (30%, 2 mL) product **3ai** (375 mg, 0.66 mmol, 36%) was obtained as yellowish solid after column chromatography (silica, ethyl acetate : hexanes = 1:1). $^{31}P\{^1H\}$ NMR (162 MHz, $CDCl_3$): δ = 19.2 (s) ppm. ^1H NMR (400 MHz, CD_2Cl_2): δ = 8.14 (d, J=7.7 Hz, 2H), 7.94 (dd, J=12.7, 8.3 Hz, 2H), 7.68 (dd, J=8.4, 2.3 Hz, 2H), 7.48-7.39 (m, 4H), 7.30 (ddd, J=7.4, 7.4, 1.1 Hz, 2H), 6.91 (d, J=2.0 Hz, 2H), 2.85 (t, J=7.6 Hz, 4H), 1.69 (tt, J=7.6, 7.6 Hz, 4H), 1.42 (qt, J=7.6, 7.3 Hz, 4H), 0.95 (t, J=7.3 Hz, 6H) ppm. $^{13}C\{^1H\}$ NMR (100 MHz, CD_2Cl_2): δ = 150.8 (d, J_{CP}=14.4 Hz), 144.4 (d, J_{CP}=24.6 Hz), 141.9 (d, J_{CP}=3.2 Hz), 140.8 (s), 137.6 (d, J_{CP}=112.7 Hz), 133.2 (d, J_{CP}=12.3 Hz), 130.2 (d, J_{CP}=107.3 Hz), 127.4 (d, J_{CP}=13.0 Hz), 126.7 (s), 124.2 (s), 122.9 (d, J_{CP}=14.6 Hz), 121.0 (s), 120.9 (s), 110.3 (s), 34.2 (s), 30.6 (s), 22.7 (s), 14.1 (s) ppm. Calculated: m/z 565.16574 $[M]^+$, 566.17357 $[M+H]^+$, 588.15551 $[M+Na]^+$. Found: MS (ESI): m/z 565.16518 $[M]^+$, 566.17259 $[M+H]^+$, 588.15436 $[M+Na]^+$.

4-(3-(9*H*-Carbazol-9-yl)phenyl)-4*H*-phospholo[3,2-*b*:4,5-*b*']dithiophene 4-oxide (3b). Starting from **2** (1.41 g, 4.4 mmol) in diethylether, *n*-BuLi (3.49 mL, 2.5 M), **1b** (1.50 g, 4.4 mmol) and H_2O_2 (30%, 2 mL) product **3b** (0.81 g, 1.8 mmol, 41%) was obtained as light yellowish solid after column chromatography (silica, ethyl acetate). $^{31}P\{^1H\}$ NMR (162 MHz, $CDCl_3$): δ = 17.8 (s) ppm. ^1H NMR (400 MHz, CD_2Cl_2): δ = 8.12 (d, J=7.8 Hz, 2H), 7.89-7.81 (m, 2H), 7.79-7.75 (m, 1H), 7.73-7.68 (m, 1H),

7.41-7.36 (m, 4H), 7.32-7.23 (m, 6H) ppm. ^{13}C {^{1}H} NMR (100 MHz, CD_2Cl_2): δ = 146.5 (d, J_{CP}=24.5 Hz), 140.9 (s), 139.3 (d, J_{CP}=112.7 Hz), 138.9 (d, J_{CP}=15.7 Hz), 133.3 (d, J_{CP}=105.8 Hz), 131.2 (d, J_{CP}=14.0 Hz), 131.1 (d, J_{CP}=2.7 Hz), 130.2 (d, J_{CP}=10.3 Hz), 129.5 (d, J_{CP}=15.1 Hz), 129.2 (d, J_{CP}=12.2 Hz), 126.6 (s), 126.3 (d, J_{CP}=14.6 Hz), 124.0 (s), 120.8(8) (s), 120.8(5) (s), 110.0 (s) ppm. Calculated: m/z 453.04054 $[M]^+$, 454.04837 $[M+H]^+$, 476.03031 $[M+Na]^+$. Found: MS (ESI): m/z 453.04004 $[M]^+$, 454.04705 $[M+H]^+$, 476.02881 $[M+Na]^+$.

4-(3-(9*H*-Carbazol-9-yl)phenyl)-2,6-dibutyl-4*H*-phospholo[3,2-*b*:4,5-*b*']dithiophene 4-oxide (3bi). Starting from **2i** (1.39 g, 3.2 mmol) in diethylether, *n*-BuLi (2.56 mL, 2.5 M), **1b** (1.10 g, 3.2 mmol) and H_2O_2 (30%, 2 mL) product **3bi** (0.55 g, 1.0 mmol, 30%) was obtained as light yellowish solid after column chromatography (silica, ethyl acetate : hexanes = 1:1). ^{31}P {^{1}H} NMR (162 MHz, $CDCl_3$): δ = 19.1 (s) ppm. ^{1}H NMR (400 MHz, CD_2Cl_2): δ = 8.13 (d, J=7.3 Hz, 2H), 7.91-7.67 (m, 4H), 7.41-7.35 (m, 2H), 7.33-7.26 (m, 4H) 6.90-6.88 (m, 2H), 2.84-2.79 (m, 4H), 1.70-1.61 (m, 4H), 1.44-1.34 (m, 4H), 0.94-0.89 (m, 6H) ppm. ^{13}C {^{1}H} NMR (100 MHz, CD_2Cl_2): δ = 150.9 (d, J_{CP}=14.4 Hz), 144.4 (d, J_{CP}=24.5 Hz), 140.9 (s), 138.8 (d, J_{CP}=15.3 Hz), 137.4 (d, J_{CP}=112.8 Hz), 133.9 (d, J_{CP}=104.3 Hz), 131.1 (d, J_{CP}=13.8 Hz), 130.8 (d, J_{CP}=2.6 Hz), 130.2 (d, J_{CP}=10.3 Hz), 129.1 (d, J_{CP}=14.6 Hz), 126.6 (s), 124.0 (s), 122.7 (d, J_{CP}=14.6 Hz), 120.8 (s), 120.8 (s), 110.0 (s), 34.2 (s), 30.6 (s), 22.6 (s), 14.1 (s) ppm. Calculated: m/z 565.16574 $[M]^+$, 566.17357 $[M+H]^+$, 588.15551 $[M+Na]^+$. Found: MS (ESI): m/z 565.16499 $[M]^+$, 566.17241 $[M+H]^+$, 588.15411 $[M+Na]^+$.

4-(2-(9*H*-Carbazol-9-yl)phenyl)-4*H*-phospholo[3,2-*b*:4,5-*b*']dithiophene 4-oxide (3c). Starting from **2** (1.00 g, 3.1 mmol) and TMEDA (0.94 mL) in diethylether, *n*-BuLi (2.47 mL, 2.5 M), **1c** (1.06 g, 3.1 mmol) and H_2O_2 (30%, 1.5 mL) product **3c** (353 mg, 0.78 mmol, 25%) was obtained as light yellowish solid after column chromatography

(silica, ethyl acetate). ^{31}P {^{1}H} NMR (162 MHz, $CDCl_3$): δ = 12.9 (s) ppm. ^{1}H NMR (400 MHz, CD_2Cl_2): δ = 8.76 (ddd, J=13.2, 7.8, 1.7 Hz, 1H), 7.82-7.83 (m, 3H), 7.81-7.69 (m, 1H), 7.24-7.20 (m, 1H), 7.13-7.04 (m, 4H), 6.75 (dd, J= 4.9, 3.5 Hz, 2H), 6.68 (dd, J=4.9, 2.6 Hz, 2H), 6.44 (d, J=7.84 Hz, 2H) ppm. ^{13}C {^{1}H} NMR (100 MHz, CD_2Cl_2): δ = 145.8 (d, J_{CP}=25.5 Hz), 142.4 (s), 138.9 (d, J_{CP}=6.1 Hz), 137.2 (d, J_{CP}=115.6 Hz), 137.2 (d, J_{CP}=7.3 Hz), 134.6 (d, J_{CP}=2.3 Hz), 132.8 (d, J_{CP}=101.8 Hz), 132.0 (d, J_{CP}=7.7 Hz), 130.4 (d, J_{CP}=11.3 Hz), 128.3 (d, J_{CP}=15.3 Hz), 126.1 (s), 125.4 (d, J_{CP}=15.3 Hz), 123.4 (s), 120.2 (s), 120.0 (s), 110.2 (s) ppm. Calculated: m/z 453.04054 $[M]^+$, 454.04837 $[M+H]^+$, 476.03031 $[M+Na]^+$. Found: MS (ESI): m/z 453.03945 $[M]^+$, 454.04731 $[M+H]^+$, 476.02871 $[M+Na]^+$.

4-(2-(9*H*-Carbazol-9-yl)phenyl)-2,6-dibutyl-4*H*-phospholo[3,2-*b*:4,5-*b*']dithiophene 4-oxide (3ci). Starting from **2i** (1.00 g, 2.3 mmol) and TMEDA (0.69 mL) in THF, *n*-BuLi (1.83 mL, 2.5 M), **1c** (0.79 g, 2.3 mmol) and H_2O_2 (30%, 1.5 mL) product **3ci** (220 mg, 0.39 mmol, 17%) was obtained as light yellowish solid after column chromatography (silica, ethyl acetate : hexanes = 1:1). ^{31}P {^{1}H} NMR (162 MHz, $CDCl_3$): δ = 14.1 (s) ppm. ^{1}H NMR (400 MHz, CD_2Cl_2): δ = 8.70 (ddd, J=13.2, 7.9, 1.5 Hz, 1H), 7.90-7.81 (m, 3H), 7.75-7.73 (m, 1H), 7.18 (dd, J=6.8, 5.9 Hz, 1H), 7.14-7.08 (m, 4H), 6.49-6.45 (m, 2H), 6.34 (d, J=2.2 Hz, 2H), 2.55-2.42 (m, 4H), 1.53-1.44 (m, 4H), 1.34 (qt, J=7.5, 7.5 Hz, 4H), 0.92 (t, J=7.5 Hz, 6H) ppm. ^{13}C {^{1}H} NMR (100 MHz, CD_2Cl_2): δ = 149.6 (d, J_{CP}=14.8 Hz), 144.0 (d, J_{CP}=25.3 Hz), 142.5 (s), 138.9 (d, J_{CP}=5.4 Hz), 137.1 (d, J_{CP}=6.9 Hz), 135.9 (d, J_{CP}=116.0 Hz), 134.3 (d, J_{CP}=2.3 Hz), 133.5 (d, J_{CP}=100.3 Hz), 131.8 (d, J_{CP}=7.7 Hz), 130.3 (d, J_{CP}=11.0 Hz), 125.7 (s), 123.5 (s), 122.1 (d, J_{CP}=14.6 Hz), 120.1 (s), 120.0 (s), 110.5 (s) 33.7 (s), 30.3 (s), 22.8 (s), 14.1 (s) ppm. Calculated: m/z 565.16574 $[M]^+$, 566.17357 $[M+H]^+$, 588.15551 $[M+Na]^+$. Found: MS (ESI): m/z 565.16504 $[M]^+$, 566.17275 $[M+H]^+$, 588.15397 $[M+Na]^+$.

4-(3-(3,6-Di-*tert*-butyl-9*H*-carbazol-9-yl)phenyl)-4*H*-phospholo[3,2-*b*:4,5-*b*']dithiophene 4-oxide (3d). Starting from **2** (0.62 g, 1.9 mmol) and TMEDA (0.58 mL) in THF, *n*-BuLi (1.53 mL, 2.5 M), **1d** (0.87 g, 1.9 mmol) and H_2O_2 (30%, 1 mL) product **3d** (185 mg, 0.33 mmol, 17%) was obtained as light yellowish solid after column chromatography (silica, DCM : MeCN = 20:1). ^{31}P $\{^1H\}$ NMR (162 MHz, $CDCl_3$): δ = 18.0 (s) ppm. ^1H NMR (400 MHz, CD_2Cl_2): δ = 8.13 (d, J=1.9 Hz, 2H), 7.86-7.74 (m, 3H), 7.68 (ddd, J=7.7, 7.7, 3.7 Hz, 1H), 7.44 (dd, J=8.7, 1.8 Hz, 2H), 7.38 (dd, J=4.9, 3.5 Hz, 2H), 7.26-7.22 (m, 4H), 1.45 (s, 18H) ppm. ^{13}C $\{^1H\}$ NMR (100 MHz, CD_2Cl_2): δ = 146.6 (d, J_{CP}=24.1 Hz), 144.0 (s), 139.4 (d, J_{CP}=15.9 Hz), 139.2 (d, J_{CP}=112.7 Hz), 139.2 (s), 132.9 (d, J_{CP}=105.8 Hz), 131.1 (d, J_{CP}=14.0 Hz), 130.7 (d, J_{CP}=2.8 Hz), 129.6 (d, J_{CP}=10.4 Hz), 129.5 (d, J_{CP}=15.2 Hz), 128.8 (d, J_{CP}=12.2 Hz), 126.4 (d, J_{CP}=14.5 Hz), 124.3 (s), 124.0 (s), 116.9 (s), 109.4 (s), 35.2 (s), 32.3 (s) ppm. Calculated: m/z 565.16574 $[M]^+$, 566.17357 $[M+H]^+$, 588.15551 $[M+Na]^+$. Found: MS (ESI): m/z 565.16500 $[M]^+$, 566.17249 $[M+H]^+$, 588.15648 $[M+Na]^+$.

4-(3-(3,6-Di-*tert*-butyl-9*H*-carbazol-9-yl)phenyl)-2,6-dibutyl-4*H*-phospholo[3,2-*b*:4,5-*b*']dithiophene 4-oxide (3di). Starting from **2i** (0.83 g, 1.9 mmol) and TMEDA (0.58 mL) in THF, *n*-BuLi (1.53 mL, 2.5 M), **1d** (0.87 g, 1.9 mmol) and H_2O_2 (30%, 1 mL) product **3di** (0.47 g, 0.7 mmol, 36%) was obtained as light yellowish solid after column chromatography (silica, DCM : MeCN = 20:1). ^{31}P $\{^1H\}$ NMR (162 MHz, $CDCl_3$): δ = 19.2 (s) ppm. ^1H NMR (400 MHz, CD_2Cl_2): δ = 8.13 (d, J=1.8 Hz, 2H), 7.88-7.73 (m, 3H), 7.68 (ddd, J=7.6, 7.6, 3.5 Hz, 1H), 7.43 (dd, J=8.7, 1.9 Hz, 2H), 7.25 (d, J=8.6 Hz, 2H), 6.89-6.88 (m, 2H), 2.82 (t, J=7.6 Hz, 4H), 1.67 (tt, J=7.6, 7.6 Hz, 4H), 1.45-1.34 (m, 22H), 0.92 (t, J=7.3 Hz, 6H) ppm. ^{13}C $\{^1H\}$ NMR (100 MHz, CD_2Cl_2): δ = 150.9 (d, J_{CP}=14.1 Hz), 144.5 (d, J_{CP}=24.5 Hz), 143.9 (s), 139.3 (d, J_{CP}=15.3 Hz), 139.2 (s), 137.3 (d, J_{CP}=112.6 Hz), 133.6 (d, J_{CP}=105.0 Hz), 131.0 (d,

J_{CP}=13.9 Hz), 130.4 (d, J_{CP}=3.7 Hz), 129.7 (d, J_{CP}=10.1 Hz), 128.6 (d, J_{CP}=12.4 Hz), 124.3 (s), 124.0 (s), 122.7 (d, J_{CP}=13.8 Hz), 116.9 (s), 109.5 (s), 35.2 (s), 34.2 (s), 32.3 (s), 30.6 (s), 22.7 (s), 14.1 (s) ppm. Calculated: m/z 677.29094 $[M]^+$, 678.29877 $[M+H]^+$, 700.28071 $[M+Na]^+$. Found: MS (ESI): m/z 677.28998 $[M]^+$, 678.29816 $[M+H]^+$, 700.27997 $[M+Na]^+$.

4-(Indolo[3,2,1-*jk*]carbazol-2-yl)-4*H*-phospholo[3,2-*b*:4,5-*b*']dithiophene 4-oxide (3e). Starting from **2** (0.50 g, 1.5 mmol) in THF, *n*-BuLi (1.22 mL, 2.5 M), **1e** (0.52 g, 1.5 mmol) and H_2O_2 (30%, 2 mL) product **3e** (73 mg, 0.16 mmol, 11%) was obtained as light yellowish solid after column chromatography (silica, DCM : MeCN = 5:1). $^{31}P\{^1H\}$ NMR (162 MHz, $CDCl_3$): δ = 22.2 (s) ppm. ^1H NMR (400 MHz, CD_2Cl_2): δ = 8.46 (d, J=13.0 Hz, 2H), 8.15 (d, J=7.8 Hz, 2H), 7.95 (d, J=7.9 Hz, 2H), 7.62 (dd, J=7.7, 7.7 Hz, 2H), 7.43-7.36 (m, 4H), 7.20 (dd, J= 4.8, 2.3 Hz, 2H) ppm. $^{13}C\{^1H\}$ NMR (100 MHz, CD_2Cl_2): δ = 146.3 (d, J_{CP}=2.3 Hz), 146.2 (d, J_{CP}=23.6 Hz), 140.8 (d, J_{CP}=111.0 Hz), 139.7 (s), 129.8 (s), 129.2 (d, J_{CP}=14.6 Hz), 128.2 (s), 126.4 (d, J_{CP}=14.5 Hz), 124.1 (s), 123.9 (d, J_{CP}=108.1 Hz), 123.0 (s), 122.9 (d, J_{CP}=14.5 Hz), 119.5 (d, J_{CP}=17.5 Hz), 113.0 (s) ppm. Calculated: m/z 451.02489 $[M]^+$, 452.03272 $[M+H]^+$, 474.01466 $[M+Na]^+$. Found: MS (ESI): m/z 451.02445 $[M]^+$, 452.03177 $[M+H]^+$, 474.01384 $[M+Na]^+$.

4-(Indolo[3,2,1-*jk*]carbazol-2-yl)-2,6-dibutyl-4*H*-phospholo[3,2-*b*:4,5-*b*']dithiophene 4-oxide (3ei). Starting from **2i** (0.97 g, 2.2 mmol) in THF, *n*-BuLi (1.78 mL, 2.5 M), **1e** (0.76 g, 2.2 mmol) and H_2O_2 (30%, 2 mL) product **3ei** (152 mg, 0.27 mmol, 12%) was obtained as light yellowish solid after column chromatography (silica, DCM : MeCN = 20:1). $^{31}P\{^1H\}$ NMR (162 MHz, $CDCl_3$): δ = 23.3 (s) ppm. ^1H NMR (400 MHz, CD_2Cl_2): δ = 8.45 (d, J=12.9 Hz, 2H), 8.15 (d, J=7.9 Hz, 2H), 7.94 (d, J=8.2 Hz, 2H), 7.61 (dd, J=7.7, 7.7 Hz, 2H), 7.40 (dd, J=7.7, 7.7 Hz, 2H), 6.85 (s, 2H), 2.82 (t, J=7.5 Hz, 4H), 1.66 (tt, J=7.5, 7.5 Hz, 4H), 1.39 (qt, J=7.5, 7.4 Hz, 4H),

0.92 (t, J=7.4 Hz, 6H) ppm. ^{13}C {^{1}H} NMR (100 MHz, CD_2Cl_2): δ = 150.6 (d, J_{CP}=13.9 Hz), 146.3 (d, J_{CP}=2.3 Hz), 144.0 (d, J_{CP}=23.7 Hz), 139.7 (s), 138.9 (d, J_{CP}=111.2 Hz), 129.8 (s), 128.2 (s), 124.7 (d, J_{CP}=106.6 Hz), 124.1 (s), 123.0 (s), 122.9 (d, J_{CP}=14.6 Hz), 122.8 (d, J_{CP}=14.2 Hz), 119.4 (d, J_{CP}=16.9 Hz), 113.0 (s), 34.2 (s), 30.6 (s), 22.6 (s), 14.1 (s) ppm. Calculated: m/z 563.15009 $[M]^+$, 564.15792 $[M+H]^+$, 586.13986 $[M+Na]^+$. Found: MS (ESI): m/z 563.14933 $[M]^+$, 564.15704 $[M+H]^+$, 586.13880 $[M+Na]^+$.

3.3) Computational Details

Density-Functional-Theory (DFT) and Time-Dependent (TD) DFT calculations have been carried out at the B3LYP/6-31+G(d) level of theory using the GAUSSIAN 09 suite of programs.[57]

3.4) Single Crystal Diffraction

Crystals of **3c**[49] suitable for single crystal diffraction were selected under a polarizing microscope, embedded in perfluorinated oil and attached to Kapton® mounts. Intensity data were collected in a dry stream of nitrogen at 100 K on a Bruker KAPPA APEX II diffractometer system. Since automatic unit-cell determination failed, reflection position were analyzed using the RLATT[60] tool. Two monoclinic domains related by reflection at (101) could be identified. They were integrated concurrently using SAINT-Plus[60] with overlap detection (HKLF5-style output file) and an empirical absorption correction using the multi-scan approach implemented in TWINABS[60] was applied. The crystal structures were solved by charge-flipping implemented in SUPERFLIP[61] and refined against *F* with the JANA2006[62] software package. The non-H atoms were refined with anisotropic displacement parameters (ADPs). The H atoms were placed at calculated positions and refined as riding on the parent C atoms. More details on data collection and refinement are summarized in the ESI.

4) Conclusion

In summary, the synthesis and characterization of novel dithienophosphole oxide donor-acceptor materials, applying various phenylcarbazole and indolocarbazole derivatives, has been presented. The following major conclusion can be drawn:

(1) The intramolecular charge transfer through the phosphorous atom can be virtually suppressed by reducing the donor strength in the donor-acceptor scaffold;

(2) Compounds potentially suitable as host materials in PhOLED applications could be obtained (triplet energies up to 2.87 eV; singlet-triplet splitting of 0.18 eV);

(3) Through space interactions have been established for the *ortho*-phenylcarbazole structure.

The theoretical calculations support the aforementioned assumptions drawn from the experimental data.

As a result, the approach of increasing the planarization of the triarylamine type donor in stepwise fashion and, thus, decreasing the donor strength clearly broadens the scope of potential applications of the dithienophosphole oxide scaffold.

Acknowledgement

T.B. thanks the Natural Sciences and Engineering Research Council of Canada (NSERC) and the Canada Foundation for Innovation for financial support. This work was supported in part by the Vienna University of Technology research funds, the Austrian Federal Ministry of Science, Research and Economy and the Swiss National Science Foundation. The X-ray centre of the Vienna University of Technology is acknowledged for providing access to the single-crystal diffractometer. K. Föttinger is acknowledged for assisting the photo-physical analysis. The student exchange of H.P. was financially supported by the Joint Study Grant (TASSEP for Canada, 2012) and the KUWI Grant (Vienna University of Technology, 2013)

References

1. S. Reineke, M. Thomschke, B. Lüssem and K. Leo, *Rev. Mod. Phys.*, 2013, **85**, 1245-1293.
2. M. Zhu and C. Yang, *Chem. Soc. Rev.*, 2013, **42**, 4963-4976.
3. Y. Tao, K. Yuan, T. Chen, P. Xu, H. H. Li, R. F. Chen, C. Zheng, L. Zhang and W. Huang, *Adv. Mater.*, 2014, **26**, 7931-7958.
4. Q. Meng, H. L. Dong, W. P. Hu and D. B. Zhu, *J. Mater. Chem.*, 2011, **21**, 11708-11721.
5. C. A. Di, F. J. Zhang and D. B. Zhu, *Adv. Mater.*, 2013, **25**, 313-330.
6. L. Torsi, M. Magliulo, K. Manoli and G. Palazzo, *Chem. Soc. Rev.*, 2013, **42**, 8612-8628.
7. Y. J. Cheng, S. H. Yang and C. S. Hsu, *Chem. Rev.*, 2009, **109**, 5868-5923.
8. A. Facchetti, *Chem. Mater.*, 2011, **23**, 733-758.
9. J. G. Mei, Y. Diao, A. L. Appleton, L. Fang and Z. N. Bao, *J. Am. Chem. Soc.*, 2013, **135**, 6724-6746.
10. Z. M. Hudson and S. N. Wang, *Acc. Chem. Res.*, 2009, **42**, 1584-1596.
11. F. Jakle, *Chem. Rev.*, 2010, **110**, 3985-4022.
12. C. R. Wade, A. E. J. Broomsgrove, S. Aldridge and F. P. Gabbai, *Chem. Rev.*, 2010, **110**, 3958-3984.
13. J. W. Chen and Y. Cao, *Macromol. Rapid Commun.*, 2007, **28**, 1714-1742.
14. J. Ohshita, *Macromol. Chem. Phys.*, 2009, **210**, 1360-1370.
15. B. C. Schroeder, Z. G. Huang, R. S. Ashraf, J. Smith, P. D'Angelo, S. E. Watkins, T. D. Anthopoulos, J. R. Durrant and I. McCulloch, *Adv. Funct. Mater.*, 2012, **22**, 1663-1670.
16. X. M. He and T. Baumgartner, *R. Soc. Chem. Adv.*, 2013, **3**, 11334-11350.
17. A. A. Jahnke and D. S. Seferos, *Macromol. Rapid Commun.*, 2011, **32**, 943-951.
18. T. Baumgartner and R. Reau, *Chem. Rev.*, 2006, **106**, 4681-4727.
19. J. Crassous and R. Reau, *Dalton Trans.*, 2008, 6865-6876.
20. Y. Matano and H. Imahoria, *Org. Biomol. Chem.*, 2009, **7**, 1258-1271.
21. S. O. Jeon and J. Y. Lee, *J. Mater. Chem.*, 2012, **22**, 4233-4243.
22. Y. Ren and T. Baumgartner, *Dalton Trans.*, 2012, **41**, 7792-7800.
23. C. Romero-Nieto and T. Baumgartner, *Synlett*, 2013, **24**, 920-937.
24. T. Baumgartner, *Acc. Chem. Res.*, 2014, **47**, 1613-1622.
25. M. G. Hobbs and T. Baumgartner, *Eur. J. Inorg. Chem.*, 2007, 3611-3628.
26. T. Baumgartner, W. Bergmans, T. Karpati, T. Neumann, M. Nieger and L. Nyulaszi, *Chem. Eur. J.*, 2005, **11**, 4687-4699.
27. Y. Dienes, S. Durben, T. Karpati, T. Neumann, U. Englert, L. Nyulaszi and T. Baumgartner, *Chem. Eur. J.*, 2007, **13**, 7487-7500.
28. M. Stolar and T. Baumgartner, *New J. Chem.*, 2012, **36**, 1153-1160.
29. C. J. Chua, Y. Ren and T. Baumgartner, *Org. Lett.*, 2012, **14**, 1588-1591.
30. C. J. Chua, Y. Ren and T. Baumgartner, *Organometallics*, 2012, **31**, 2425-2436.
31. C. J. Chua, Y. Ren, M. Stolar, S. Xing, T. Linder and T. Baumgartner, *Eur. J. Inorg. Chem.*, 2014, **2014**, 1767-1774.
32. T. Baumgartner, T. Neumann and B. Wirges, *Angew. Chem. Int. Ed.*, 2004, **43**, 6197-6201.
33. S. Durben, Y. Dienes and T. Baumgartner, *Org. Lett.*, 2006, **8**, 5893-5896.
34. C. Romero-Nieto, S. Durben, I. M. Kormos and T. Baumgartner, *Adv. Funct. Mater.*, 2009, **19**, 3625-3631.
35. C. Romero-Nieto, K. Kamada, D. T. Cramb, S. Merino, J. Rodriguez-Lopez and T. Baumgartner, *Eur. J. Inorg. Chem.*, 2010, 5225-5231.
36. C. Romero-Nieto, M. Marcos, S. Merino, J. Barbera, T. Baumgartner and J. Rodriguez-Lopez, *Adv. Funct. Mater.*, 2011, **21**, 4088-4099.
37. Y. Ren, W. H. Kan, V. Thangadurai and T. Baumgartner, *Angew. Chem. Int. Ed.*, 2012, **51**, 3964-3968.
38. G. S. He, L.-S. Tan, Q. Zheng and P. N. Prasad, *Chem. Rev.*, 2008, **108**, 1245-1330.
39. Y. Tao, C. Yang and J. Qin, *Chem. Soc. Rev.*, 2011, **40**, 2943-2970.
40. A. Mishra and P. Bäuerle, *Angew. Chem. Int. Ed.*, 2012, **51**, 2020-2067.
41. Y. Shirota and H. Kageyama, *Chem. Rev.*, 2007, **107**, 953-1010.
42. X. Cai, A. B. Padmaperuma, L. S. Sapochak, P. A. Vecchi and P. E. Burrows, *Appl. Phys. Lett.*, 2008, **92**, 083308-1 - 083308-3.
43. S. O. Jeon, K. S. Yook, C. W. Joo and J. Y. Lee, *Adv. Funct. Mater.*, 2009, **19**, 3644-3649.
44. H.-H. Chou and C.-H. Cheng, *Adv. Mater.*, 2010, **22**, 2468-2471.
45. P. K. Koech, E. Polikarpov, J. E. Rainbolt, L. Cosimbescu, J. S. Swensen, A. L. Von Ruden and A. B. Padmaperuma, *Org. Lett.*, 2010, **12**, 5534-5537.

46. U. S. Bhansali, E. Polikarpov, J. S. Swensen, W.-H. Chen, H. Jia, D. J. Gaspar, B. E. Gnade, A. B. Padmaperuma and M. A. Omary, *Appl. Phys. Lett.*, 2009, **95**, 233304-1 - 233304-3.
47. P. Kautny, Diploma Thesis, Vienna University of Technology, 2013.
48. E. Mondal, W.-Y. Hung, H.-C. Dai and K.-T. Wong, *Adv. Funct. Mater.*, 2013, **23**, 3096-3105.
49. (**3c**): $C_{26}H_{16}NOPS_2$, *M*r = 453.50, *T* = 100 K, monoclinic, space group $P2_1$, *a* = 8.3295(6) Å, *b* = 14.1464(10) Å, *c* = 8.8132(6) Å, β = 103.1530(19)°, *V* = 1011.24(12) $Å^3$, *Z* = 2, *ρ*calcd = 1.4894 Mgm^{-3}, *μ* = 0.363 mm^{-1}, *λ* = 0.71070 Å, *θmax* = 32.72°, 82676 measured reflections, 7360 [*R*(int) = 0.0407] independent reflections, GOF on *F* = 1.92, R_1 = 0.0198, wR_2 = 0.0272 ($I>3\sigma(I)$), R_1 = 0.0201, wR_2 = 0.0273 (all data), largest difference peak and hole 0.280 and -0.200 $eÅ^{-3}$. Twinned by twofold rotation about [10-1] with a 63.75:36.25(7) volume ratio. CCDC reference number 1407916.
50. H. H. Li, Y. Wang, K. Yuan, Y. Tao, R. F. Chen, C. Zheng, X. H. Zhou, J. F. Li and W. Huang, *Chem. Commun.*, 2014, **50**, 15760-15763.
51. C. Romero-Nieto, S. Merino, J. Rodriguez-Lopez and T. Baumgartner, *Chem. Eur. J.*, 2009, **15**, 4135-4145.
52. P. Kautny, D. Lumpi, Y. Wang, A. Tissot, J. Bintinger, E. Horkel, B. Stöger, C. Hametner, H. Hagemann, D. Ma and J. Fröhlich, *J. Mater. Chem. C*, 2014, **2**, 2069-2081.
53. A. Chaskar, H.-F. Chen and K.-T. Wong, *Adv. Mater.*, 2011, **23**, 3876-3895.
54. C. Adachi, M. A. Baldo, M. E. Thompson and S. R. Forrest, *J. Appl. Phys.*, 2001, **90**, 5048-5051.
55. Q. Zhang, B. Li, S. Huang, H. Nomura, H. Tanaka and C. Adachi, *Nat. Photonics*, 2014, **8**, 326-332.
56. H. Uoyama, K. Goushi, K. Shizu, H. Nomura and C. Adachi, *Nature*, 2012, **492**, 234-238.
57. M. J. Frisch, G. W. Trucks, H. B. Schlegel, G. E. Scuseria, M. A. Robb, J. R. Cheeseman, J. A. Jr. Montgomery, T. Vreven, K. N. Kudin, J. C. Burant, J. M. Millam, S. S. Iyengar, J. Tomasi, V. Barone, B. Mennucci, M. Cossi, G. Scalmani, N. Rega, G. A. Petersson, H. Nakatsuji, M. Hada, M. Ehara, K. Toyota, R. Fukuda, J. Hasegawa, M. Ishida, T. Nakajima, Y. Honda, O. Kitao, H. Nakai, M. Klene, X. Li, J. E. Knox, H. P. Hratchian, J. B. Cross, V. Bakken, C. Adamo, J. Jaramillo, R. Gomperts, R. E. Stratmann, O. Yazyev, A. J. Austin, R. Cammi, C. Pomelli, J. W. Ochterski, P. Y. Ayala, K. Morokuma, G. A. Voth, P. Salvador, J. J. Dannenberg, V. G. Zakrzewski, S. Dapprich, A. D. Daniels, M. C. Strain, O. Farkas, D. K. Malick, A. D. Rabuck, K. Raghavachari, J. B. Foresman, J. V. Ortiz, Q. Cui, A. G. Baboul, S. Clifford, J. Cioslowski, B. B. Stefanov, G. Liu, A. Liashenko, P. Piskorz, I. Komaromi, R. L. Martin, D. J. Fox, T. Keith, M. A. Al-Laham, C. Y. Peng, A. Nanayakkara, M. Challacombe, P. M. W. Gill, B. Johnson, W. Chen, M. W. Wong, C. Gonzalez and J. A. Pople, Gaussian 09, Revision A.02, Gaussian, Inc.: Wallingford CT, **2009**.
58. J. Ohshita, M. Nodono, H. Kai, T. Watanabe, A. Kunai, K. Komaguchi, M. Shiotani, A. Adachi, K. Okita, Y. Harima, K. Yamashita and M. Ishikawa, *Organometallics*, 1999, **18**, 1453-1459.
59. Y. Ren, Y. Dienes, S. Hettel, M. Parvez, B. Hoge and T. Baumgartner, *Organometallics*, 2009, **28**, 734-740.
60. Bruker Analytical X-ray Instruments, Inc., Madinson, WI, USA: SAINT and SADABS 2008.
61. L. Palatinus and G. Chapuis, *J. Appl. Crystallogr.*, 2007, **40**, 786-790.
62. V. Petříček, M. Dušek, L. Palatinus, *Z. Kristallogr.,* 2014, **229**, 345.